

文章编号:1671-1637(2012)02-0046-07

## 无外界动力源主动悬架的能量可用性

陈士安,王勇刚,王东,何仁,刘红光

(江苏大学汽车与交通工程学院,江苏镇江 212013)

**摘要:**将无外界动力源的主动悬架在半主动模式下吸收平均功率与在主动模式下消耗平均功率的绝对值比作为能量可用性的评价指标,分析了优化PID与LQG控制主动悬架的性能与能量可用性。针对某重型汽车的1/4车主动悬架模型,设计了PID与LQG控制器。当悬架阻尼比为0.1时,以悬架二次型性能指标为目标函数,利用遗传算法对PID控制器参数进行了优化。发现优化PID控制主动悬架的二次型性能指标较LQG控制主动悬架大3.32%,优化PID与LQG控制主动悬架的能量可用性评价指标分别为17.15和226.33。分析结果表明:LQG控制主动悬架的性能略优于优化PID控制主动悬架;2种主动悬架均满足能量可用性要求,且LQG控制主动悬架的能量可用性远优于优化PID控制主动悬架。

**关键词:**汽车工程;主动悬架;无外界动力源;能量可用性;比例-微分-积分控制;线性二次型控制  
**中图分类号:**U463.33 **文献标志码:**A

### Energy availability of active suspension without external energy supply

CHEN Shi-an, WANG Yong-gang, WANG Dong, HE Ren, LIU Hong-guang

(School of Automotive and Traffic Engineering, Jiangsu University, Zhenjiang 212013, Jiangsu, China)

**Abstract:** The absolute ratio of mean power reclaimed in the semi-active control mode divided by the value consumed in the active control mode was proposed as the evaluating index of energy availability for active suspension without external energy supply (ASWEES). The performance and energy availability of ASWEES were analyzed based on optimized PID and LQG controllers, which were designed for a quarter-heavy-vehicle ASWEES. When the damping ratio was 0.1, PID control parameters were optimized by using the genetic algorithm with suspension quadratic performance index taken as the objective function. It is pointed that the suspension quadratic performance index of ASWEES based on optimized PID control is 3.32% bigger than the index based on LQG control, and their energy availability indexes are 17.15 and 226.33 respectively. The result indicates that the performance of ASWEES based on LQG control is weakly better, two ASWEESs meet the demand of energy availability, and the energy availability of ASWEES based on LQG control is strongly better. 6 tabs, 8 figs, 20 refs.

**Key words:** automotive engineering; active suspension; no external energy supply; energy availability; PID control; LQG control

## 0 Introduction

The active and semi-active suspensions are used to

improve vehicle ride comfort<sup>[1-8]</sup>. It is usually believed that the performance of active suspension is more excellent than that of semi-active

**Receipt Date:** 2011-12-22

**Research Projects:** National Natural Science Foundation of China (50805066)

**Author Resume:** CHEN Shi-an(1973-), Male, Jingzhou, Hubei, Associate Professor of Jiangsu University, PhD, Research on Automotive Technology of Vibration Analysis and Control, Energy Conservation and Active Safety, +86-511-88791872, chenshian73@ujs.edu.cn.



suspension. It is well known that the manufacturing and using costs of active suspension are higher than that of semi-active one because external power source and active force actuators are needed by the active suspension [3-8]. The energy conservation suspension technology is one of automotive research focuses [9-12]. Yu, et al analyzed the energy saving potential of electromagnetic energy regenerative suspension [13-14], and pointed that the suspension could recover some vibration energy. In fact, the suspension is a kind of semi-active suspensions. Huang, et al studied an electrical energy-regenerative suspension, and designed its main-loop controller with two modes, consumptive full-active (CFA) mode and regenerative semi-active (RSA) mode [11,15]. The former mode addresses sprung mass vibration control, however, the latter mode emphasizes energy regeneration. In fact, the suspension with CFA mode is a full-active suspension, and the suspension with RSA mode is a semi-active suspension.

Based on the suspension reclaiming energy [12], a new active suspension without external energy supply (ASWEES) is given. The character of ASWEES is that the reclaiming energy under the semi-active control mode is used to actively reduce vibration under the active control mode. So ASWEES needs no external energy supply. The energy availability is one of key questions for ASWEES. It is a necessary condition for ASWEES being feasible that the reclaiming energy under the semi-active control mode meets the energy demand to actively reduce vibration under the active control mode. Bigger is the value of the reclaiming power under the semi-active control mode subtracted by the power need to actively reduce vibration under the active control mode, better is the energy availability of ASWEES.

To investigate the energy availability of ASWEES, LQG and optimized PID controllers are designed for ASWEES based on a quarter-heavy-vehicle suspension model [16-20]. Comparative analysis on the ride comfort and energy availability of ASWEES using the two controllers is carried out.

## 1 Working principle and model of ASWEES

### 1.1 Working principle and model

Fig. 1 shows the working principle of ASWEES. When the direction of control force is contrary to that of relative velocity of sprung mass to unsprung mass, ASWEES is working in the semi-active control mode, and the reclaiming energy/active cylinder turns the suspension vibration into the hydraulic energy of the accumulator. When the direction of control force is the same as that of relative velocity of sprung mass to unsprung mass, ASWEES is working in the active control mode, and the accumulator gives actively reducing vibration energy to the suspension by the reclaiming energy/active cylinder. During a pulse-width-modulation (PWM) cycle, the actively reducing force or the semi-active damping force can be gotten when solenoid valves receive the corresponding PWM control signals from the control unit. According to Newton Second Law, the differential equations for ASWEES are written as follows

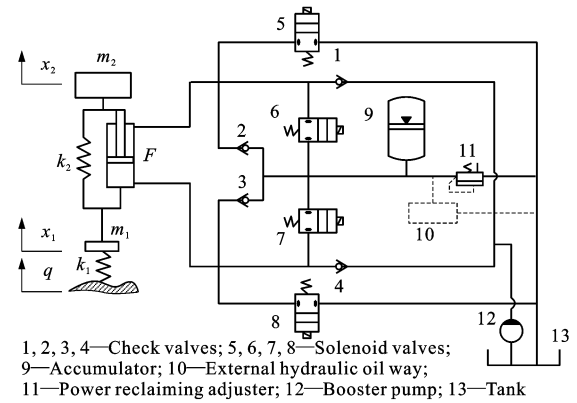


Fig. 1 Working principle of ASWEES

$$\begin{cases} m_1 \ddot{x}_1 = -k_1(x_1 - q) + k_2(x_2 - x_1) + c_0(\dot{x}_2 - \dot{x}_1) - F \\ m_2 \ddot{x}_2 = -k_2(x_2 - x_1) - c_0(\dot{x}_2 - \dot{x}_1) + F \end{cases} \quad (1)$$

$$\dot{q} = 2\pi n_0 w \sqrt{G_q(n_0)} u - 2\pi f_0 q \quad (2)$$

Where  $m_1$  is unsprung mass;  $m_2$  is sprung mass;  $k_1$  is tire stiffness;  $k_2$  is suspension stiffness;  $F$  is control force in general;  $c_0$  is basal damping;  $q$  is the displacement input of suspension;  $n_0$  is reference spatial frequency and equals  $0.1 \text{ m}^{-1}$ ;  $w$  is road white-noise signal;  $G_q(n_0)$  is road



roughness coefficient and is determined by road class;  $u$  is vehicle velocity;  $f_0$  is lower cut off frequency and equals  $0.011u$ ;  $x_1$  is the vertical displacement of unsprung mass;  $x_2$  is the vertical displacement of sprung mass.

Suspension system's state vector is

$$\mathbf{X} = (q, x_1, x_2, x_3, x_4)^T$$

$$x_3 = \dot{x}_1, x_4 = \dot{x}_2$$

Its state-space model is

$$\dot{\mathbf{X}} = \mathbf{A}\mathbf{X} + \mathbf{B}\mathbf{U} + \mathbf{G}\mathbf{W} \quad (3)$$

$$\mathbf{A} = \begin{bmatrix} -2\pi f_0 & 0 & 0 & 0 & 0 \\ 0 & 0 & 0 & 1 & 0 \\ 0 & 0 & 0 & 0 & 1 \\ \frac{k_1}{m_1} & -\frac{k_1+k_2}{m_1} & \frac{k_2}{m_1} & -\frac{c_0}{m_1} & \frac{c_0}{m_1} \\ 0 & \frac{k_2}{m_2} & -\frac{k_2}{m_2} & \frac{c_0}{m_2} & -\frac{c_0}{m_2} \end{bmatrix}$$

$$\mathbf{B} = \begin{bmatrix} 0 & 0 & 0 & -\frac{1}{m_1} & \frac{1}{m_2} \end{bmatrix}^T$$

$$\mathbf{G} = \begin{bmatrix} 2\pi n_0 \sqrt{G_q(n_0)u} & 0 & 0 & 0 & 0 \end{bmatrix}^T$$

$$\mathbf{U} = [F], \mathbf{W} = [\omega]$$

## 1.2 Evaluating index of ride comfort and energy availability

Suspension quadratic performance index is adopted as follow

$$J = \frac{1}{T} \int_0^T (a_2^2 + \delta'_1 F_d^2 + \delta_2 f_d^2) dt \quad (4)$$

Where  $a_2$  is the acceleration of sprung mass and equals  $\ddot{x}_2$ ;  $F_d$  is the dynamic load of unsprung mass and equals  $k_1(x_1 - q)$ ;  $f_d$  is suspension deflection and equals  $x_2 - x_1$ ;  $\delta'_1$  is the weight of  $F_d^2$ ;  $\delta_2$  is the weight of  $f_d^2$ ;  $T$  is the total running time of vehicle;  $t$  is time variable.

When  $F_d$  is taken by  $x_1 - q$ ,  $J$  is

$$J = \frac{1}{T} \int_0^T [\ddot{x}_2^2 + \delta_1 (x_1 - q)^2 + \delta_2 (x_2 - x_1)^2] dt \quad (5)$$

Where  $\delta_1$  is the weight of  $(x_1 - q)^2$ .

$P$  is the power of reclaiming energy/active cylinder

$$P = F(\dot{x}_2 - \dot{x}_1) \quad (6)$$

When  $P > 0$ , the accumulator gives actively reducing vibration energy to the suspension by the reclaiming energy/active cylinder. When  $P < 0$ , the reclaiming energy/active cylinder turns the

suspension vibration into the hydraulic energy of the accumulator.

$P_s$  is the mean power of the reclaiming energy/active cylinder in the semi-active control mode;  $P_a$  is the mean power in the active control mode

$$\begin{cases} P_s = \frac{W_s}{T} = \frac{1}{T} \int_0^T P dt & P < 0 \\ P_a = \frac{W_a}{T} = \frac{1}{T} \int_0^T P dt & P > 0 \end{cases} \quad (7)$$

Where  $W_s$  is the work of the reclaiming energy/active cylinder in the semi-active control mode;  $W_a$  is the work in the active control mode.

Obviously,  $P_s$  is positive and  $P_a$  is negative.

When  $\left| \frac{P_s}{P_a} \right| = 1$ , the reclaiming energy under the semi-active control mode justly meets the energy demand to actively reduce vibration under the active control mode in the ideal condition. Here,  $\left| \frac{P_s}{P_a} \right|$  is proposed as the evaluating index for the

energy availability of ASWEES. Bigger is  $\left| \frac{P_s}{P_a} \right|$ ,

Better is the energy availability of ASWEES.

## 1.3 Confirming $\delta_1$ and $\delta_2$

The ASWEES is reformed as a heavy vehicle passive suspension<sup>[12]</sup>. When  $u$  is  $20 \text{ m} \cdot \text{s}^{-1}$  on an ISO C-class road, the parameters of passive suspension and road inputs are shown in Tab. 1. Here,  $c$  is the shock absorber damping of passive suspension.

Tab. 1 Parameters of passive suspension and road inputs

Parameter	Value	Parameter	Value
$m_1/\text{kg}$	350	$k_1/(\text{N} \cdot \text{m}^{-1})$	$3.0 \times 10^6$
$m_2/\text{kg}$	5 000	$k_2/(\text{N} \cdot \text{m}^{-1})$	$5.05 \times 10^5$
$c/(\text{N} \cdot \text{s} \cdot \text{m}^{-1})$	30 150	$G_q(n_0)/(\text{m}^2 \cdot \text{m}^{-1})$	$2.56 \times 10^{-4}$
$f_0/\text{Hz}$	0.22		

According to Ref. [20],  $\delta_1$  and  $\delta_2$  are expressed as follows

$$\begin{cases} \delta_1 = \beta_1 \gamma_1 \\ \delta_2 = \beta_2 \gamma_2 \end{cases} \quad (8)$$

$$\sigma^2(a_2) = \beta_1 \sigma^2(x_1 - q) = \beta_2 \sigma^2(f_d) \quad (9)$$

$$W_1 = \frac{W_2}{\gamma_1} = \frac{W_3}{\gamma_2} \quad (10)$$

$$W_1 + W_2 + W_3 = 1$$

Where  $\beta_1$  and  $\beta_2$  are the normalizing coefficients of



$(x_1 - q)^2$  and  $f_d^2$  relative to  $a_2^2$  respectively;  $\gamma_1$  and  $\gamma_2$  are the subjective weights of  $(x_1 - q)^2$  and  $f_d^2$  respectively when the weight of  $a_2^2$  is 1;  $\sigma^2(a_2)$ ,  $\sigma^2(x_1 - q)$  and  $\sigma^2(f_d)$  are the variances of  $a_2$ ,  $x_1 - q$  and  $f_d$  respectively;  $W_1$ ,  $W_2$  and  $W_3$  are the subjective weights of  $a_2$ ,  $x_1 - q$  and  $f_d$  respectively, and are gotten according to the relative importances of  $a_2$ ,  $x_1 - q$  and  $f_d$ .

Under the frequently-used condition of heavy vehicle, the importance of  $a_2$  over  $f_d$ , the strong importance of  $a_2$  over  $x_1 - q$ , and the weak importance of  $x_1 - q$  over  $f_d$  are demonstrated. The subjective weights are obtained in Tab. 2.

Tab. 2 Subjective weights

$W_1$	$W_2$	$W_3$	$\gamma_1$	$\gamma_2$
0.649 1	0.279 0	0.071 9	0.429 8	0.110 8

$\sigma^2(a_2)$ ,  $\sigma^2(x_1 - q)$  and  $\sigma^2(f_d)$  are gotten by simulation on the passive suspension based on ODE3 solving method of Matlab software listed in Tab. 3. According to Eq. (9), Tab. 1 and Tab. 3,  $\beta_1$ ,  $\beta_2$ ,  $\delta_1$  and  $\delta_2$  are obtained in Tab. 4.

Tab. 3  $\sigma^2(a_2)$ ,  $\sigma^2(x_1 - q)$  and  $\sigma^2(f_d)$

$\sigma^2(a_2)/(\text{m} \cdot \text{s}^{-2})^2$	$\sigma^2(x_1 - q)/\text{m}^2$	$\sigma^2(f_d)/\text{m}^2$
4.516 2	$1.847 5 \times 10^{-5}$	$1.557 7 \times 10^{-4}$

Tab. 4 Proportional coefficients and weights

Coefficient	Value	Weight	Value
$\beta_1$	2 444	$\delta_1$	105 060
$\beta_2$	27 081	$\delta_2$	3 000.6

## 2 Optimization and design of PID controller

### 2.1 Design of PID controller

The structure of PID controller for ASWEES is shown in Fig. 2, and its output is

$$F_p = k_p e + k_i \int e dt + k_d \frac{de}{dt} \quad (11)$$

$$e = r - y \quad (12)$$

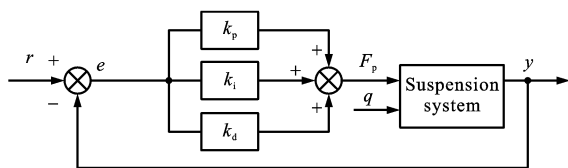


Fig. 2 Structure of PID controller

Where  $F_p$  is the control force of ASWEES based on PID control;  $k_p$ ,  $k_i$  and  $k_d$  are the proportional

gain, the integral gain and the derivative gain respectively;  $e$  is the error input of PID controller;  $r$  is the desired acceleration of sprung mass;  $y$  is the acceleration output of sprung mass and equals  $\ddot{x}_2$ .

### 2.2 Optimization of PID control parameters

Genetic algorithm (GA) is chosen as the optimizing method for  $k_p$ ,  $k_i$  and  $k_d$  of PID controller for ASWEES<sup>[18]</sup>. During the optimization procedure, GA iteratively manipulates the populations of the chromosomes using reproduction, crossover and mutation operations, and evaluates the suitability of each solution using a fitness function. Here, the optimization objective function  $J$  is taken as the fitness function. The chromosomes with good fitness are carried forward into the next generation and are subsequently used as the basis for generating new and improved solutions. The search procedure continues iteratively until the specified termination conditions have been satisfied. Here, the termination conditions are that the solutions with desired fitness are satisfied for the specified numbers of generations. The flow chart for the optimization based on GA is shown in Fig. 3.

The optimization procedure is carried out by simulation. Simulation time length is set as 40 s and ODE3 solving method is employed.  $c_0$  is set as  $10^4 \text{ N} \cdot \text{s} \cdot \text{m}^{-1}$  to decrease the consuming power of basal damping and to insure a good ride comfort. That is to say that the suspension damping ratio is equal to 0.1.

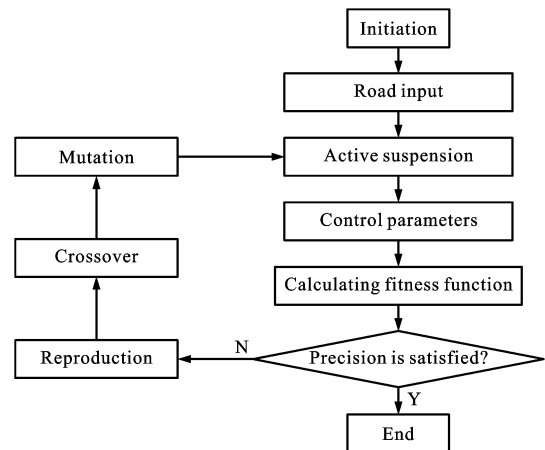


Fig. 3 Optimization flow of PID controller parameters



GA optimizing parameters and PID controller parameters are listed in Tab. 5.  $J$ -G (number of generation) curve is shown in Fig. 4. When the optimizing generation reaches 27, the optimum value of  $J$  is obtained and equals 4.580 9. The optimizing results are  $k_p=760.556$ ,  $k_i=116.410$ , and  $k_d=0.0032$ .

Tab. 5 Parameter settings

Parameter	Value	Parameter	Value
Max number of generation	50	Mutation rate	0.017 5
Initial population size	60	Scope of $k_p$	[0, 20 000]
Crossover rate	0.7	Scope of $k_i$	[0, 200 000]
Generation gap	0.9	Scope of $k_d$	[0, 10]

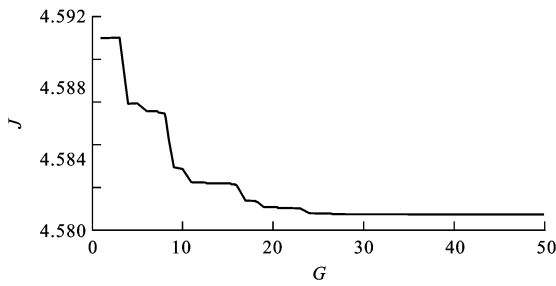


Fig. 4  $J$ -G curve

### 3 Design of LQG controller

#### 3.1 LQG controller

The standard form of  $J$  is expressed as follow

$$J = \frac{1}{T} \int_0^T (\mathbf{X}^T \mathbf{Q} \mathbf{X} + \mathbf{U}^T \mathbf{R} \mathbf{U} + 2\mathbf{X}^T \mathbf{N} \mathbf{U}) dt \quad (13)$$

$$\mathbf{N} = \begin{bmatrix} 0 & \frac{k_2}{m_2^2} & -\frac{k_2}{m_2^2} & \frac{c_0}{m_2^2} & -\frac{c_0}{m_2^2} \end{bmatrix}^T$$

$$\mathbf{R} = \begin{bmatrix} \frac{1}{m_2^2} \end{bmatrix}$$

$$\mathbf{Q} = \begin{bmatrix} \delta_1 & -\delta_1 & 0 & 0 & 0 \\ -\delta_1 & \delta_1 + \delta_2 + \frac{k_2^2}{m_2^2} & -\delta_2 - \frac{k_2^2}{m_2^2} & \frac{k_2 c_0}{m_2^2} & -\frac{k_2 c_0}{m_2^2} \\ 0 & -\delta_2 - \frac{k_2^2}{m_2^2} & \delta_2 + \frac{k_2^2}{m_2^2} & -\frac{k_2 c_0}{m_2^2} & \frac{k_2 c_0}{m_2^2} \\ 0 & \frac{k_2 c_0}{m_2^2} & -\frac{k_2 c_0}{m_2^2} & \frac{c_0^2}{m_2^2} & -\frac{c_0^2}{m_2^2} \\ 0 & -\frac{k_2 c_0}{m_2^2} & \frac{k_2 c_0}{m_2^2} & -\frac{c_0^2}{m_2^2} & \frac{c_0^2}{m_2^2} \end{bmatrix}$$

According to modern control theory, the minimum of  $J$  can be obtained when the control force is

$$\mathbf{F}_1 = -\mathbf{R}^{-1}(\mathbf{S}\mathbf{B} + \mathbf{N})^T \mathbf{X} \quad (14)$$

$\mathbf{S}$  is the solution of Ricatti equation as follow

$$(\mathbf{S}\mathbf{A})^T + \mathbf{S}\mathbf{A} - (\mathbf{S}\mathbf{B} + \mathbf{N})\mathbf{R}^{-1}(\mathbf{S}\mathbf{B} + \mathbf{N})^T + \mathbf{Q} = \mathbf{0} \quad (15)$$

$\mathbf{F}_1$  is usually written as follow

$$\mathbf{F}_1 = -\mathbf{Y}\mathbf{X} \quad (16)$$

Where  $\mathbf{Y}$  is the feedback gain matrix of LQG controller and can be obtained by using LQR function of Matlab software as follow

$$(\mathbf{Y}, \mathbf{S}, \mathbf{E}) = \text{L}(\mathbf{A}, \mathbf{B}, \mathbf{Q}, \mathbf{R}, \mathbf{N}) \quad (17)$$

Where  $\mathbf{E}$  is the system eigenvector;  $\text{L}(\cdot)$  is LQR function.

#### 3.2 Parameters of LQG controller

Eqs. (15)-(17) show that  $c_0$  influences  $\mathbf{F}_1$ . In addition,  $c_0$  influences the power consuming of ASWEES. So it is necessary to investigate the influence of  $c_0$  on the performance and power consuming of ASWEES.  $\mathbf{A}$  and  $\mathbf{Q}$  can be written as follows

$$\mathbf{A} = \mathbf{A}_0 + \mathbf{R}^{-1} \mathbf{B} \mathbf{N}^T \quad (18)$$

$$\mathbf{Q} = \mathbf{Q}_0 + \mathbf{R}^{-1} \mathbf{N} \mathbf{N}^T \quad (19)$$

$$\mathbf{A}_0 = \begin{bmatrix} -2\pi f_0 & 0 & 0 & 0 & 0 \\ 0 & 0 & 0 & 1 & 0 \\ 0 & 0 & 0 & 0 & 1 \\ \frac{k_1}{m_1} & -\frac{k_1}{m_1} & 0 & 0 & 0 \\ 0 & 0 & 0 & 0 & 0 \end{bmatrix} \quad (20)$$

$$\mathbf{Q}_0 = \begin{bmatrix} \delta_1 & -\delta_1 & 0 & 0 & 0 \\ -\delta_1 & \delta_1 + \delta_2 & -\delta_2 & 0 & 0 \\ 0 & -\delta_2 & \delta_2 & 0 & 0 \\ 0 & 0 & 0 & 0 & 0 \\ 0 & 0 & 0 & 0 & 0 \end{bmatrix} \quad (21)$$

Taking Eqs. (18) and (19) into Eq. (15), there is an equation as follow

$$[\mathbf{S}(\mathbf{A}_0 + \mathbf{R}^{-1} \mathbf{B} \mathbf{N}^T)]^T + \mathbf{S}(\mathbf{A}_0 + \mathbf{R}^{-1} \mathbf{B} \mathbf{N}^T) - (\mathbf{S}\mathbf{B} + \mathbf{N})\mathbf{R}^{-1}(\mathbf{S}\mathbf{B} + \mathbf{N})^T + \mathbf{Q}_0 + \mathbf{R}^{-1} \mathbf{N} \mathbf{N}^T = \mathbf{0}$$

It is simplified as follow

$$\mathbf{A}_0^T \mathbf{S}^T + \mathbf{S}\mathbf{A}_0 - \mathbf{R}^{-1} \mathbf{S}\mathbf{B}(\mathbf{S}\mathbf{B})^T + \mathbf{Q}_0 = \mathbf{0} \quad (22)$$

Taking Eqs. (14), (18) and (19) into Eq. (13), there is an equation as follow

$$\begin{aligned} \mathbf{X}^T \mathbf{Q} \mathbf{X} + \mathbf{U}^T \mathbf{R} \mathbf{U} + 2\mathbf{X}^T \mathbf{N} \mathbf{U} = & \mathbf{X}^T [\mathbf{Q}_0 + \mathbf{R}^{-1} \mathbf{N} \mathbf{N}^T + \\ & \mathbf{R}^{-1}(\mathbf{S}\mathbf{B} + \mathbf{N})\mathbf{R}\mathbf{R}^{-1}(\mathbf{S}\mathbf{B} + \mathbf{N})^T - \\ & 2\mathbf{N}\mathbf{R}^{-1}(\mathbf{S}\mathbf{B} + \mathbf{N})^T] \mathbf{X} \end{aligned}$$

It is simplified as follow

$$\begin{aligned} \mathbf{X}^T \mathbf{Q} \mathbf{X} + \mathbf{U}^T \mathbf{R} \mathbf{U} + 2\mathbf{X}^T \mathbf{N} \mathbf{U} = \\ \mathbf{X}^T [\mathbf{Q}_0 + \mathbf{R}^{-1} \mathbf{S}\mathbf{B}(\mathbf{S}\mathbf{B})^T] \mathbf{X} \end{aligned} \quad (23)$$

Because  $k_2$  and  $c_0$  do not appear in Eq. (22),  $\mathbf{S}$  is irrelative to  $k_2$  and  $c_0$ . Similarly, Eqs. (13) and



(23) show the responses of ASWEES based on LQG control are irrelative to  $k_2$  and  $c_0$  too. Smaller is  $c_0$ , smaller is its power consuming. So  $c_0$  is set as 0. According to Eq.(17),  $\mathbf{Y}$  is obtained as follow

$$\mathbf{Y} = 10^5 (3.475\ 6, -0.738\ 9, -2.311\ 1, -0.166\ 2, 0.549\ 3)$$

#### 4 Performance and energy availability of ASWEES

Based on the results of sections 2-3, the evaluating indexes of performance and energy availability of ASWEES based on optimized PID control and LQG control are gotten.  $J$ ,  $P_s$ ,  $P_a$ ,  $\sigma(a_2)$ ,  $\sigma(x_1 - q)$  and  $\sigma(f_d)$  are listed in Tab. 6.  $\sigma(a_2)$ ,  $\sigma(x_1 - q)$  and  $\sigma(f_d)$  are the mean square roots of  $a_2$ ,  $x_1 - q$  and  $f_d$  respectively.  $J$ - $t$  curves are shown in Fig. 5.  $P$ - $t$  curves of ASWEES based on optimized PID control are shown in Fig. 6.  $P$ - $t$  curves of ASWEES based on optimized LQG control are shown in Fig. 7.  $W_s/W_a$ - $t$  curves are shown in Fig. 8.

Tab. 6 Data of  $\sigma(a_2)$ ,  $\sigma(x_1 - q)$ ,  $\sigma(f_d)$ ,  $J$ ,  $P_s$  and  $P_a$

Parameter	Optimized PID control	LQG control
$\sigma(a_2) / (\text{m} \cdot \text{s}^{-2})$	1.228 8	1.380 3
$\sigma(f_d) / \text{m}$	0.014 2	0.012 9
$\sigma(x_1 - q) / \text{m}$	0.004 8	0.004 4
$J$	4.580 9	4.428 6
$P_s / \text{kW}$	-1.179 2	-2.919 6
$P_a / \text{kW}$	0.068 4	0.128 9

Tab. 6 and Fig. 5 show that  $J$  values of ASWEES based on LQG control and optimized PID control are 4.428 6 and 4.580 9 respectively, it is to say that  $J$  of ASWEES based on LQG control is 3.32% smaller than that of ASWEES based on optimized PID control. So the performance of ASWEES based on LQG control is weakly better than that of the other.

Figs. 6-8 show that the reclaiming energy powers and works in the semi-active control mode are bigger than the energy consuming powers and works in the active control mode.  $P_s$  is strongly bigger than  $P_a$  for ASWEES based on LQG control.

According to Tab. 6,  $\left| \frac{P_s}{P_a} \right|$  values of ASWEES based on optimized PID control and LQG control are

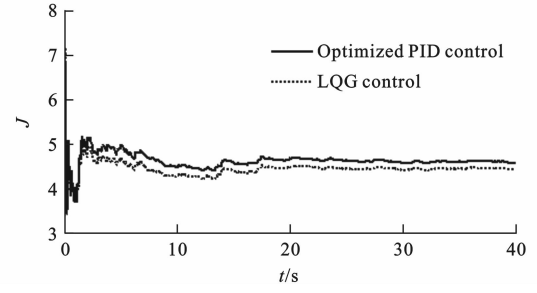


Fig. 5  $J$ - $t$  curves

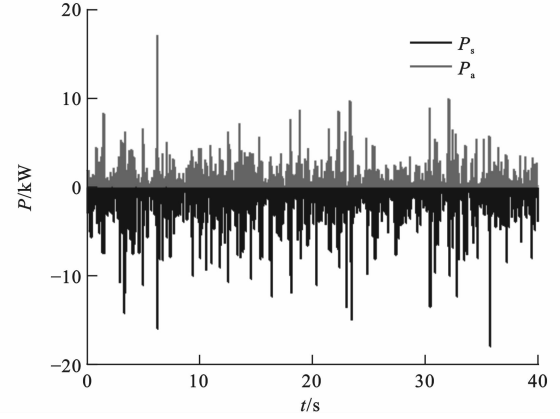


Fig. 6  $P$ - $t$  curves based on optimized PID control

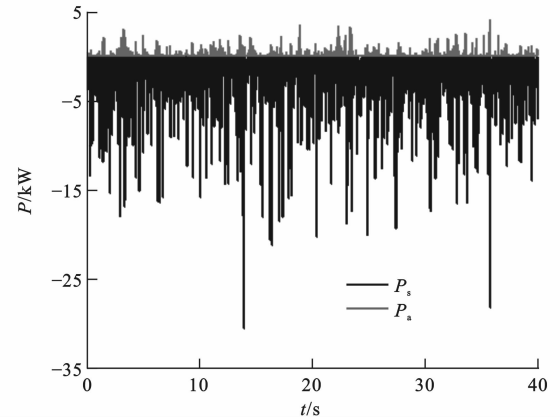


Fig. 7  $P$ - $t$  curves based on LQG control

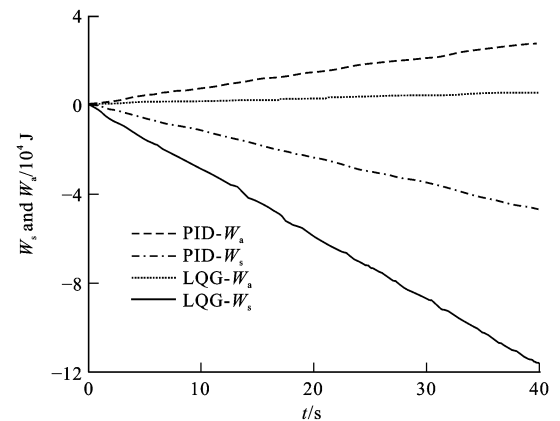


Fig. 8 Curves of  $W_s/W_a$ - $t$



obtained and equal to 17.15 and 226.33 respectively. So the energy availabilities of two ASWEESs meet the demand, and the energy availability of ASWEES based on LQG control is much better than that of the other.

## 5 Conclusions

The absolute ratio of mean power reclaimed in the semi-active control mode divided by that consumed in the active control mode is proposed as the energy availability index of ASWEES. Bigger is the index, better is the energy availability. The parameters of PID controller are optimized according to GA with suspension quadratic performance index taken as the fitness function when the suspension damping ratio is 0.1. The suspension performance of ASWEES based on LQG control is weakly better than that of ASWEES based on optimized PID control. The energy availabilities of two ASWEESs meet the demand, and the energy availability of ASWEES based on LQG control is much better than that of the other.

## References:

- [1] ZAREH S H, SARRAFAN A, KHAYYAT A A, et al. Intelligent semi-active vibration control of eleven degrees of freedom suspension system using magnetorheological dampers[J]. Journal of Mechanical Science and Technology, 2012, 26(2): 323-334.
- [2] CREWS J H, MATTSO M G, BUCKNER G D. Multi-objective control optimization for semi-active vehicle suspensions[J]. Journal of Sound and Vibration, 2011, 330(23): 5502-5516.
- [3] MALEKSHAHI A, MIRZAEI M. Designing a non-linear tracking controller for vehicle active suspension systems using an optimization process [J]. International Journal of Automotive Technology, 2012, 13(2): 263-271.
- [4] YIM S. Design of a robust controller for rollover prevention with active suspension and differential braking[J]. Journal of Mechanical Science and Technology, 2012, 26(1): 213-222.
- [5] LIU Shu-bo, ZHAO Ding-xuan.  $H_{\infty}$ /generalized  $H_2$  static output feedback control method for active suspension[J]. China Journal of Highway and Transport, 2009, 22(4): 122-126.
- [6] EBRAHIMI B, BOLANDHEMMAT H, KHAMESE M B, et al. A hybrid electromagnetic shock absorber for active vehicle suspension systems[J]. Vehicle System Dynamics, 2011, 49(1/2): 311-332.
- [7] RYU S, KIM Y, PARK Y. Robust  $H_{\infty}$  preview control of an active suspension system with norm-bounded uncertainties[J]. International Journal of Automotive Technology, 2008, 9(5): 585-592.
- [8] GAO Hui-jun, SUN Wei-chao, SHI Peng. Robust sampled-data  $H_{\infty}$  control for vehicle active suspension systems[J]. IEEE Transactions on Control Systems Technology, 2010, 18(1): 238-245.
- [9] DAVID S B, BOBROVSKY B Z. Actively controlled vehicle suspension with energy regeneration capabilities[J]. Vehicle System Dynamics, 2011, 49(6): 833-854.
- [10] MONTAZERI-GH M, SOLEYMANI M. Investigation of the energy regeneration of active suspension system in hybrid electric vehicles[J]. IEEE Transactions on Industrial Electronics, 2010, 57(3): 918-925.
- [11] HUANG K, YU F, ZHANG Y. Active controller design for an electromagnetic energy-regenerative suspension[J]. International Journal of Automotive Technology, 2011, 12(6): 877-885.
- [12] CHEN Shi-an, HE Ren, LU Sen-lin. New reclaiming energy suspension and its working principle[J]. Chinese Journal of Mechanical Engineering, 2007, 43(11): 177-182.
- [13] YU Chang-miao, WANG Wei-hua, WANG Qing-nian. Damping characteristic and its influence factors in energy regenerative suspension[J]. Journal of Jilin University: Engineering and Technology Edition, 2010, 40(6): 1482-1486.
- [14] YU Chang-miao, WANG Wei-hua, WANG Qing-nian. Design of electromagnetic energy regenerative suspension system and analysis of energy conservation[J]. Automobile Technology, 2010(2): 21-25.
- [15] HUANG Kun, YU Fan, ZHANG Yong-chao. Active control of energy-regenerative electromagnetic suspension based on energy flow analysis[J]. Journal of Shanghai Jiaotong University, 2011, 45(7): 1068-1073.
- [16] TAO Yong-hua. Application of New PID Control[M]. 2<sup>nd</sup> Edition. Beijing: China Machine Press, 2003.
- [17] ZENG Jie-ru, GU Zheng-qi, LI Wei-ping, et al. A research on the fuzzy PID control for vehicle semi-active suspension based on genetic algorithm[J]. Automotive Engineering, 2010, 32(5): 429-433.
- [18] WANG Chen, WANG Shi-cheng. Parameters setting of PID controller based on genetic algorithm[J]. Computer Simulation, 2005, 22(10): 112-114, 143.
- [19] JIN Y, YU D J. Adaptive neuron control using an integrated error approach with application to active suspensions[J]. International Journal of Automotive Technology, 2008, 9(3): 329-335.
- [20] CHEN Shi-an, QIU Feng, HE Ren, et al. A method for choosing weights in a suspension LQG control[J]. Journal of Vibration and Shock, 2008, 27(2): 65-68, 176.